Dynamic model of monovalent-divalent cation exchange in polyelectrolyte gels

Matan Mussel, Owen Lewis, Peter J. Basser, and Ferenc Horkay

Phys. Rev. Materials **6**, 035602 — Published 24 March 2022

DOI: 10.1103/PhysRevMaterials.6.035602

Dynamic model of monovalent-divalent cation exchange in polyelectrolyte gels

Matan Mussel[1,*], Owen Lewis[2], Peter J. Basser[3], and Ferenc Horkay[3]

1. Department of Physics, University of Haifa, Haifa, Israel
2. Department of Mathematics and Statistics, University of New Mexico, Albuquerque, NM, USA.
3. Eunice Kennedy Shriver National Institute of Child Health and Human Development, National Institutes of Health, Bethesda, MD, USA.
* Corresponding author: mmussel@sci.haifa.ac.il

Abstract

A multicomponent model that imposes conservation laws and constitutive relations for polymer chains, water, and ions was investigated by determining the transient changes in a negatively charged gel exposed to a solution containing both mono- and divalent cations. Association of ion exchange with gel volume is achieved by imposing a linear relation between the polymer-solvent interaction parameter and concentration of divalent cations adsorbed onto the polymer chains. Semi-quantitative agreement with measurements made on sodium polyacrylate gels is demonstrated in three aspects: (1) dynamics of gel swelling and deswelling, (2) ion partitioning coefficient, and (3) effect of crosslink density. These results imply that the multicomponent coarse-grained continuum modeling approach can be useful for quantitative predictions over macroscopic length and time scales including the description of volume transitions exhibited by these systems.

1 Introduction

Polyelectrolyte hydrogels are soft, complex media made of charged crosslinked macromolecules, solvent, and counter and co-ions organized in clouds around the polymer chains. The various competing forces (mechanical, electrical, osmotic, and chemical) give rise to a rich behavior over multiple time and length scales [1]. A steep and reversible change in volume can sometimes be observed in response to minute changes of environmental conditions, such as temperature, ionic composition, solvent quality, pH, and electric field [2]. This phenomenon was identified in living systems [3–5], and is also widely used in various man-made applications, such as sensors, actuators, and drug-delivery devices [6,7].

Many of these volume transitions occur at time and length scales that are typically larger than $\sim$1 millisecond and $\sim$1 micrometer, respectively [5,6]. Atomistic and coarse-grained molecular dynamic (MD) models, while powerful and detailed, are limited in their ability to be extended to the steady state or equilibrium regimes needed to describe these processes. The time and length scales simulated by such MD models are usually no more than $\sim$100 μs and $\sim$100 nm, respectively, and require high-performance computing [8]. Continuum models, on the other hand, can describe such systems over macroscopic time and length scales with a lower computational overhead. The mean-field simplification, however, comes at a price. Upon taking the continuum limit we might disregard important properties or features of the system. For instance, distinguishing the fluid-like characteristics of the solvent vs. the solid-like response of the polymer network. Therefore, considerations must be given to the form of the conservation and constitutive laws that define the relationships between and among the macroscopic

variables of the system. A promising continuum approach to model the dynamics of gels interacting with their environment is the multicomponent formalism, which distinctively treats the polymer network, solvent, and ions as separate entities. These models are based on traditional continuum-mechanics principles but maintain certain distinct features for each component; e.g., separate chemical potential expressions for the polymer network, solvent, and ions [9–18].

In this article we model an anionic polyelectrolyte hydrogel exposed to new ionic environment containing a mixture of monovalent and divalent cations, a common situation in multiple biological systems [5]. Many experiments have been performed to characterize equilibrium properties of gels exposed to different ionic environments, both in synthetic [19–25] and biogels [26–29]. It was previously demonstrated that the ionic environment influences multiple properties of the system, including equilibrium gel volume [19,26], ion partitioning coefficient [5], electric potential difference [30,31], elastic modulus of gel [32], mobility of solvent and ions within the gel [33], and the mean interaction between the polymer segments and solvent [20,34]. The latter implies that an ion-dependent Flory interaction parameter plays an important role in determining the equilibrium state of the system.

Indeed, a small change in the concentration of divalent cations can lead to a steep transition in the equilibrium state through the effect on the ion-dependent Flory interaction parameter [35,36]. In many applications, including in biological systems however, transient changes are just as important as the steady state behavior. Mucus, DNA, and pectin are examples of negatively charged biopolymers undergoing analog abrupt transitions when exposed to different mono- and divalent cations, and their dynamic response to the ionic environment is believed to play an important functional role *in vivo* [5]. Furthermore, models with capabilities for predicting both dynamic and equilibrium behaviors are critical for describing the behavior of mechano-chemical actuators and sensors, drug delivery systems, polymer-based MEMS, and in various biomedical and tissue engineering applications [7]. However, only few attempts have been made to connect added salt to the polymer-solvent interaction parameter and the induced transient response of the polymer chains [37].

The purpose of this paper is to demonstrate that a relatively simple multicomponent continuum model captures multiple transient and equilibrium aspects – that are potentially universal – of a polyelectrolyte gel model. The important feature in the model is a linear relation between the Flory interaction parameter and concentration of adsorbed divalent cations onto the polymer chains. We demonstrate that using this simple relation is sufficient to obtain semi-quantitative results that agree with measurements made on a polyelectrolyte gel model (sodium polyacrylate). Compatibility is achieved in three aspects: (1) dynamics of gel swelling and deswelling, (2) ion partitioning coefficient, and (3) effect of crosslink density.

2 Model Description

The model under consideration was originally developed by Keener, Fogelson, and co-workers, and is described in detail in the Supplementary Material section S1 [38] as well as in

Ref. [36]. In brief, the polyelectrolyte hydrogel is treated as a multicomponent medium that includes the polymer network, solvent, and small molecular ionic species. The states of the polymer network and solvent are described by their volume fraction and velocity fields, $\theta_n(\vec{r},t), v_n(\vec{r},t)$ and $\theta_s(\vec{r},t), v_s(\vec{r},t)$, respectively (equations S1—S6 [38] that account for the conservation of mass and momentum as well as the volume-averaged incompressibility constraint). A common assumption is that other particle species do not contribute significantly to the local volume because they have a comparatively low concentration. The polymer building blocks (monomers) are either neutral or negatively charged, while the solvent is assumed to be electrically neutral. Counter- and co-ions are described by concentration fields, $c_j(\vec{r},t)$. We use a minimal Ansatz that includes hydrogen, hydroxide, sodium, chloride, and calcium ions, $j = H^+, OH^-, Na^+, Cl^-, Ca^{2+}$, respectively. The interaction between the cationic species (H^+, Na^+, Ca^{2+}) and the polymer network is captured by crudely dividing each ionic group into two subgroups: one subgroup describing adsorbed ions that are strongly interacting with charged monomers (b_k, $k = H, Na, Ca, C2$ (which stand for HM, NaM, CaM^+, CaM_2, respectively), where $C2$ denotes the population of calcium ions paired with two adsorbing monomers [39]), and the second subgroup describing free ions that experience negligible interacting with the polymer chains (c_j). Although the mathematical formalism we use (law of mass action, equations S7—S8 [38]) is typically associated with chemical reaction kinetics, the adsorption process considered here does not involve a chemical synthesis of the ion and monomer. Rather, by adsorbed ions we mean ions that are localized (on average) in a compact cloud around the polymer chains (thickness is less than the effective Debye screening length in the solution) [27]. Nevertheless, the mathematical formalism of the law of mass action serves as a useful approximation, which captures, for instance, the rate of exchange between adsorbed and free ions. Variables of the system are summarized in table 1 along with the corresponding conservation laws (equations S1—S8 and S23 [38]).

Variable name	**Variable**	**Equation description**	**Equation number**
Polymer volume fraction	θ_n	Polymer conservation of mass	S2
Polymer velocity field	v_n	Polymer conservation of momentum	S3
Solvent volume fraction	θ_s	Solvent conservation of mass	S4
Solvent velocity field	v_s	Solvent conservation of momentum	S5
Pressure	p	Volume-averaged incompressibility constraint	S6
Concentration of adsorbed ion j	b_j	Adsorbed ion conservation of mass	S7
Concentration of free ion j	c_j	Free ion conservation of mass	S8
Electric potential field	ϕ_e	Electroneutrality constraint	S23

Table 1: list of model variables and corresponding conservation laws [38].

Additional equations include constitutive relations for the polymer network, solvent, and ions. In particular, the forces acting on the polymer network are derived from the stress tensor (equations S9) and from the free energy of the material. The latter is described as a linear sum of the entropic, elastic, short-range interactions, and electrostatic contributions (equations S11-

S15). The form of the entropic potential is derived by a mean field argument after counting configurations of particles on a lattice. The original derivation of the model [36] assumes that all particles (monomers, solvent, ions) can be placed on the same lattice. However, even if we assume that the monomers are of much larger size than ions and solvent molecules, the final entropy potential acting on the system is unchanged [40].

The novel aspect of this model – which distinguishes it from other multicomponent models [9–18] – is the assumption that the phenomenological short-range polymer-solvent interaction parameter, namely, the Flory parameter is modified by adsorption of divalent cations onto the polymer chains. An ion-dependent Flory parameter was previously demonstrated in various polyelectrolyte gels [20,34]. However, the detailed relation remains unclear. Following Keener, Fogelson, and colleagues [36] we consider the simplest, namely, a linear dependence of Flory parameter on local concentration of doubly adsorbed calcium ions:

$$\chi(b_{C2}) = \chi_0 + \chi_1(b_{C2}), \qquad \chi_1 \propto b_{C2}, \quad (1)$$

(see equations S17-S18 for more details).

An elastic term was not considered in Keener and Fogelson' previous works. Here we use the Flory-Rehner model, which accounts for crosslinking between the polymer chains to prevent infinite dilution (equation S13) [41]. The forces acting on the solvent are described by its stress tensor (equation S10) and entropic and short-range interaction expressions (equation S20). Forces acting on the ions include entropy (diffusion), electrostatic interactions (equation S22), and the ability of cations to adsorb onto the polymer chains (equations S7 and S8).

The system of equations (equations S2—S8 and S23) is solved in one spatial dimension using the finite difference numerical technique, which is described in detail in Ref. [37]. In brief, a closed container is represented by imposing no-flux boundary conditions for all species and zero Dirichlet conditions for both velocity fields. At each time step we solved the equations in the following order:

1. Given ionic concentrations (c_j and b_k, $j = H^+, Na^+, Ca^{2+}, OH^-, Cl^-$ and $k = H, Na, Ca, C2$, electric potential gradient ($\partial_x \phi_e$), and volume fractions (θ_a, $a = n, s$), we evaluate the chemical potential gradients $\partial_x \mu_a$and $\partial_x \mu_j$.
2. Given the chemical potential gradients ($\partial_x \mu_a, \partial_x \mu_j$), we solve the force-balance equations to determine the network and solvent velocities (v_a).
3. For the respective velocity fields, we solve the continuity equations and update the solvent and network volume fractions (θ_a).
4. The transport velocities and volume fractions (v_a and θ_a) are used to evolve the ionic concentrations while simultaneously solving for a new electric potential gradient ($c_j, b_k, \partial_x \phi_e$).

A dimensionless form of the equations is given in the Supplementary Materials section S2 [38], along with characteristic length and time scales, and dimensionless variables. The 23 dimensionless parameters of the model are described in the Supplementary Materials section S3 [38]. All the parameters describe quantities that have well-defined physical meaning and can be independently measured, in principle. They are required for a realistic treatment of a system

of this complexity, and generally appear in other multicomponent models [9–18]. The list of parameters includes diffusion coefficients for 5 ionic species, adsorption and desorption rates for 3 types of cations, viscosity of solvent and polymer network, drag coefficient between the solvent and network, elastic modulus of polymer network, average chain length, fraction of charged sites on polymer chains, coordination number, 4 parameters governing the short-range pairwise interaction energies, and system size (table S1 in the Supplementary Material [38]).

Important length scales are the averaged particle size, $\nu^{1/3}$ (ν is the particle volume), the size of the gel, $\ell \gg \nu^{1/3}$, and the total size of the system (gel + bath), L. Relevant time scales include the characteristic time of diffusion of the solvent, $\tau_w = \frac{\ell^2}{D_w}$, the characteristic time of ion adsorption $\tau_{k_j^+} = \frac{1}{k_j^+ c_j}$ and characteristic time of ion desorption $\tau_{k_j^-} = \frac{1}{k_j^-}$. Here, D_w is the solvent diffusion coefficient, and k_j^+ and k_j^- are the adsorption and desorption coefficients of ion j to the polymer chain, respectively.

3 Results and Discussion

To illustrate the competition between mono- and divalent cations and how their relative concentrations affect the dynamics of gel swelling, we numerically solve the dimensionless model equations (equations S29—S32, S41—S44 [38]) for a one-dimensional partially dry gel immersed in a solution containing sodium, calcium, and chloride ions with a specific pH. Figure 1a shows the initial profile of the polymer network volume fraction as a function of the spatial coordinate x normalized by the length of the total domain, L. The region with appreciable network fraction ($\theta_n = 0.5$) at the left side of the domain ($x/L < 0.15$) represents the initial gel region. The rest of the domain ($0.15 < x/L$) is the external bath solution, containing 0.3 mM $CaCl_2$, 40 mM NaCl, and pH=7.

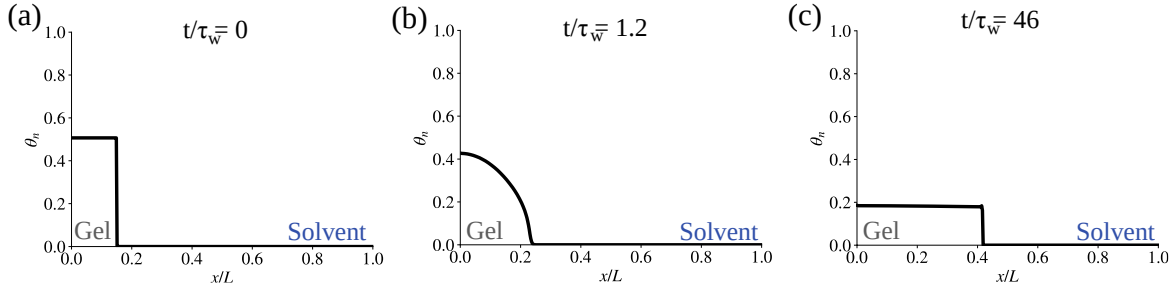

Figure 1: Polymer network volume fraction as a function of the 1D spatial coordinate x. (a) At initial state, the polymer charged groups are neutralized with sodium ions and the solvent contains 40 mM NaCl, 0.3 mM $CaCl_2$ at pH = 7. (b) volume fraction profile of the polymer network at a non-equilibrium instance (t/τ_w=1.2). (c) volume fraction of the polymer network profile at equilibrium (t/τ_w>20). Model parameters are listed in section S3 of the Supplementary Material [38].

As time evolves, solvent and ions diffuse in and out of the gel, leading to gel swelling. Figure 2b depicts a typical profile of θ_n at an intermediate time when the system is not in equilibrium with its environment. For a 1 μm gel size, $\tau_W \sim 0.1 - 1\ s$, while for a 1 mm gel size $\tau_W \sim 10 - 100$ minutes. After sufficient time ($\frac{t}{\tau_W} > 20$) the system effectively reaches equilibrium. An equilibrium profile of θ_n is shown in figure 1c. Movie S1 shows the development of $\theta_n(x,t)$ from

initial state until an equilibrium is reached. It should be noted that although the movie shows oscillations at the gel-solvent interface, these are not physical oscillations. Rather, this is a well-known numerical artifact, arising from using a Lax-Wendroff second order discretization of advection on problems that exhibit sharp interfaces [42].

The degree of swelling of the gel is defined as the ratio of the instantaneous gel volume to its volume in the dry state. For a 1D system we approximate the gel volume by calculating its cubed size at each instance of time, an approximation based on length-scale argument. Since the left edge of the cell is fixed at $x = 0$, the gel size is calculated by identifying its right edge, $x_{edge}(t)$; i.e., the point where θ_n decreases below a certain value of choice (denoted as θ_n^{crit}). Here, we use the condition $\theta_n^{crit} = 0.1$ to estimate the right edge of the gel. For instance, in figure 1a the right edge of the gel is found at $x_{edge}/L = 0.15$, while in figure 1c it is located at $x_{edge}/L \approx 0.42$. The gel volume in the dry state is estimated by calculating its boundary if the entire volume of gel was at volume fraction 1. For the scenario considered in figure 1, $x_{edge}^{dry}/L = 0.075$. Accordingly, the instantaneous degree of swelling of the gel is calculated using the relation:

$$\frac{V}{V_0} \approx \left[\frac{x_{edge}(t)}{x_{edge}^{dry}}\right]^3 \quad (2)$$

Figure 2a shows the estimated degree of swelling of the gel as a function of time for different values of initial $CaCl_2$ concentration in the external bath solution. Below a certain calcium concentration, $c_{Ca}^{init} \leq c_0$ (≈ 0.5 mM in the given example) the gel swells until it reaches equilibrium. Gel swelling results from the balance of forces, which favors network expansion at low adsorbed calcium concentration. The characteristic time scale of gel swelling is τ_w.

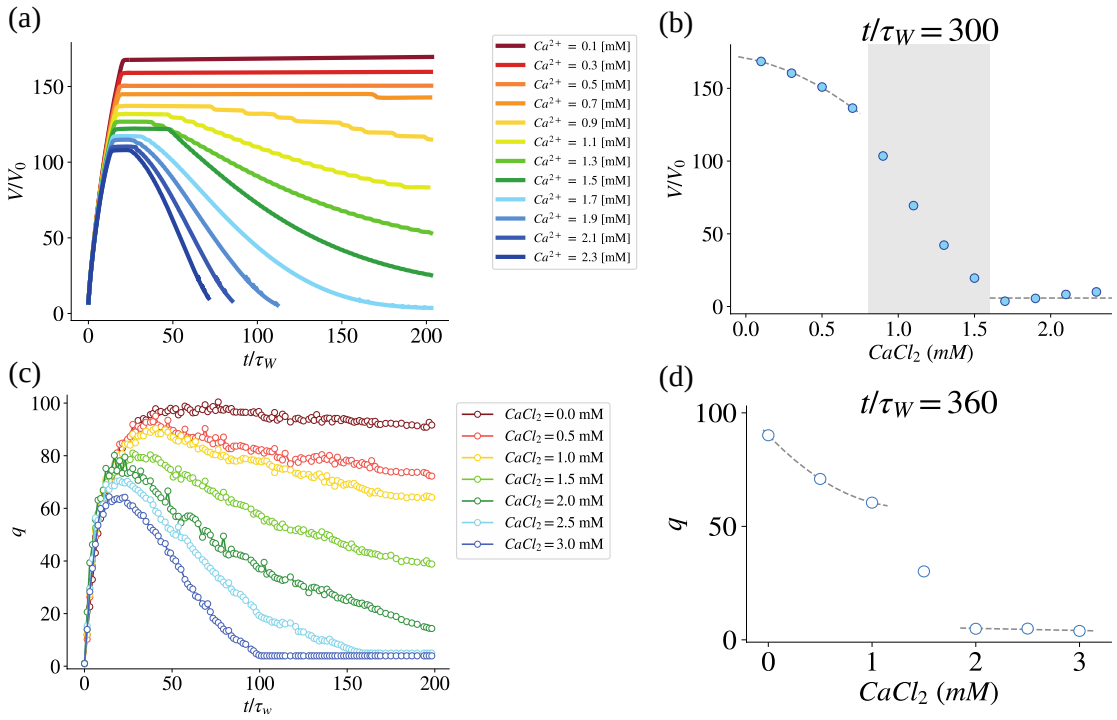

Figure 2: (a) Degree of swelling as a function of time for different initial $CaCl_2$ concentrations in the solution. Model parameters are listed in section S3 of the Supplementary Material [38]. (b) Calculation of the equilibrium degree of swelling as a function of initial $CaCl_2$ in the salt solution. Grey area indicates the region of volume transition. (c) Measured data showing the degree of swelling of sodium polyacrylate (NaPA) gels as a function of dimensionless time. (d) Equilibrium degree of swelling of NaPA gels measured after 5 days ($\frac{t}{\tau_w} = 360$).

A significantly different swelling response is observed when the initial $CaCl_2$ concentration in the external bath solution exceeds c_0. In this case, after a transient time of gel swelling the gel gradually deswells until reaching an equilibrium state. For intermediate values, $c_0 < c_{Ca}^{init} < c_1$, ($c_1 = 1.5\,mM$ in the above example) the equilibrium state of the deswollen gel is not fully collapsed, and for $c_1 \leq c_{Ca}^{init}$ the gel expels most of the water and collapses almost completely (degree of swelling lower than 5). This is shown in figure 2a and Movie S2. For high calcium concentration ($1.9\,mM \leq c_{Ca}^{init}$ in the above example) we were unable to reach equilibrium because the solvent fraction within the gel approached 0. In such a scenario, the equations of motion become nearly singular. Small amounts of numerical error can lead to $\theta_s < 0$, which causes a severe numerical instability. This is a well-known limitation of Eulerian numerical treatments of two-phase models [43]. Furthermore, the apparent unphysical decrease in polymer volume fraction at $x = 0$ arises because the simulation is not resolving the large potential gradients between the first few grid points near the boundary. Because of the *no flux* boundary condition at the left, the collapse forces at the gel interior (two grid points from the boundary) pull the network from the grid point immediately next to the boundary into the second grid point. More sophisticated numerical treatments could potentially avoid these issues.

The deswelling process is attributed to the adsorption of calcium ions onto the polyelectrolyte chains which modifies the Flory interaction parameter. The rate of this process

depends on the adsorption coefficient k_{Ca}^{+}, associated with a characteristic time scale $\tau_{Ca} = \frac{1}{k_{Ca}^{+} c_{Ca}^{init}}$. Indeed, the duration of the deswelling process decreases as the initial concentration of calcium in the solution increases (figure 2a). In the present work $\tau_{Ca} \sim (1-10)\tau_W$.

The equilibrium degree of swelling was calculated at $\frac{t}{\tau_W} = 300$, and is shown as a function of the initial $CaCl_2$ concentration in figure 2b. A gradual decrease in the degree of swelling is obtained for $c_{Ca}^{init} < c_0$. Between $c_0 < c_{Ca}^{init} < c_1$, a steeper decrease in the degree of swelling is found. At $c_1 < c_{Ca}^{init}$ the gel is fully collapsed.

Figure 2c shows swelling measurements made on cubic sodium polyacrylate (NaPA) gels starting from an initial dry state with an edge size of 1—1.5 mm^3. Gel preparation and measurement process are described in detail in Ref. [24]. The gel was immersed in a solution containing 40 mM NaCl, a varying amount of $CaCl_2$, and pH=5.5. Here, q is estimated by measuring the gel mass normalized by the mass of the dry gel, which is approximately the degree of swelling of the gel, V/V_0. Time axis is normalized using τ_W=20 minutes, estimated from the initial gel size and water diffusion coefficient. The resemblance of figures 2a and 2c is evident by the qualitative gel response (significant swelling followed by deswelling), and the similarity of the order of magnitudes of both the degree of swelling and time. Figure 2d shows the equilibrium value of NaPA gels measured after five days ($\frac{t}{\tau_W} = 360$). The volume transition model calculation resembles the experimental data in both shape and scale. Comparable equilibrium response was found also in biogels made of DNA chains [28]. This is an indication that qualitatively similar structural features can be identified in various polymer systems despite important differences, such as chain flexibility and chemical composition.

To gain a deeper understanding on the swelling process, we investigate the dynamic behavior of the Flory interaction parameter. The dimensionless parameter $\chi(x,t)$ describes the degree of segregation between the polymer network and solvent and depends linearly on the local concentration of adsorbed calcium ions, $b_{C2}(x,t)$ (equation S17) [36,37]. To analyze its dynamics during the swelling/deswelling processes, we calculate the mean value of the interaction parameter within the gel, $\bar{\chi} = <\chi>_{\frac{x}{L}<0.0125} = \frac{1}{0.0125L}\int_0^{0.0125L} \chi dx$. Figure 3a shows the evolution of $\bar{\chi}$ over time for different values of the initial calcium concentration in the external bath solution. For $c_{Ca}^{init} < c_1$, the interaction parameter remains smaller than the mean-field prediction of the theta-solvent ($\chi_\theta = \frac{1}{2}$) through the entire gel swelling process. By adsorbing calcium ions onto the polymer network the effective interaction parameter increases, leading to gel deswelling. Once $\frac{1}{2} < \bar{\chi}$, the effective interactions between the gel segments are as if they are in poor solvent conditions, leading to phase separation between the polymer network and solvent. This expected behavior matches the results of figure 2a when $c_1 < c_{Ca}^{init}$. At high concentration of calcium in the external bath solution (1.9 mM $\leq c_{Ca}^{init}$) the calculation did not reach an equilibrium value of $\bar{\chi}$ because of the numerical instability arising when θ_s approaches 0.

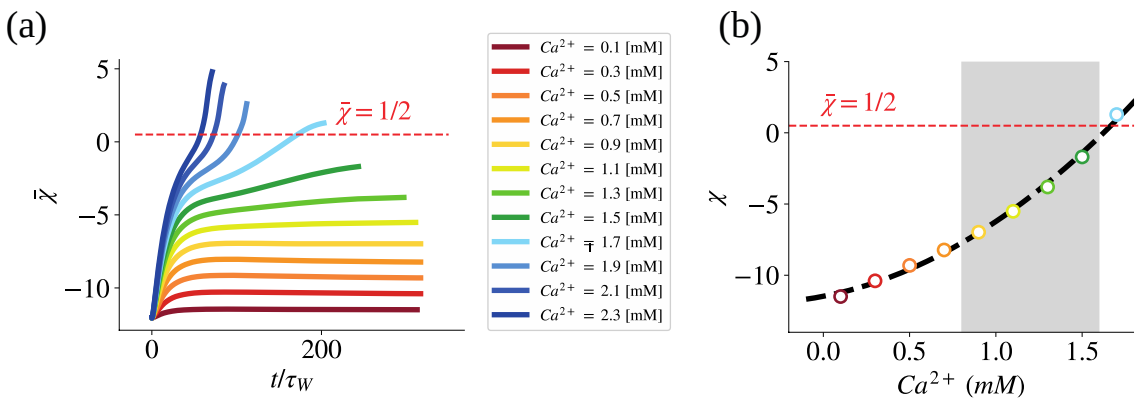

Figure 3: (a) transient change of the Flory-like interaction parameter averaged within the gel interior (x/L<0.0125) as a function of time for multiple values of the initial calcium concentration in the external bath solution, c_{Ca}. (b) Equilibrium values of the interaction parameter as a function of c_{Ca}. Grey region indicates the region of volume transition. Dashed black line is a linear fit to data: $\bar{\chi} = 2.9[CaCl_2]^2 + 2.34[CaCl_2] - 11.48$.

Figure 3b plots the equilibrium value of the average interaction parameter as a function of c_{Ca}^{init} (plotted for $c_{Ca}^{init} < 1.9\ mM$). A quadratic fit to data (dashed black line in figure 3b) yields $\bar{\chi} = \mathrm{A}_2\left(c_{Ca}^{init}\right)^2 + \mathrm{A}_1 c_{Ca}^{init} + \mathrm{A}_0 = 2.9\left(c_{Ca}^{init}\right)^2 + 2.34 c_{Ca}^{init} - 11.48$. The fit excludes results at high calcium concentration that did not reach equilibrium. The observed increase of interaction parameter is consistent with previous measurements reported for NaPA gels, where analysis of osmotic pressure measurements indicated that the Flory-Huggins interaction parameter exhibits a continuous increase with increasing calcium concentration in the external bath solution [24]. An analogy may be drawn from the typical dependence of the interaction parameter on temperature, $\chi = \frac{A}{T} + B$, where calcium ion concentration replaces the role of inverse temperature [25].

We now turn to the analysis of the ion partitioning coefficient of the gel in the multicomponent fluid model. The ion partitioning coefficient is defined as the ratio of ion concentrations within the gel interior to the external bath solution

$$P_j = \frac{c_j^{gel}}{c_j^{sol}}. \quad (3)$$

We define the calcium concentration within the gel to be a spatial average over its entire domain ($c_{Ca}^{gel} =< c_{Ca} >_{x<x_{edge}}$). Similarly, we estimate the calcium concentration within the solvent by averaging over a region well away from the gel ($c_{Ca}^{sol} =< c_{Ca} >_{0.99<\frac{x}{L}}$). The calcium partition function is calculated and plotted as a function of time in figure 4a for different values of initial calcium concentration in the external bath solution. Color code follows the legend of figure 3a. Interestingly, the calcium partition reaches an equilibrium value later than the degree of swelling. For example, at c_{Ca}^{init} ≤0.9 mM the adsorption of calcium equilibrates at (80—100)t/τ_W while the degree of swelling equilibrates already at 10—20 t/τ_W. For higher calcium concentrations (1.1 mM < c_{Ca}^{init}) longer time is needed. This observation may be explained by the slower kinetic process of calcium ion adsorption as compared to solvent diffusion.

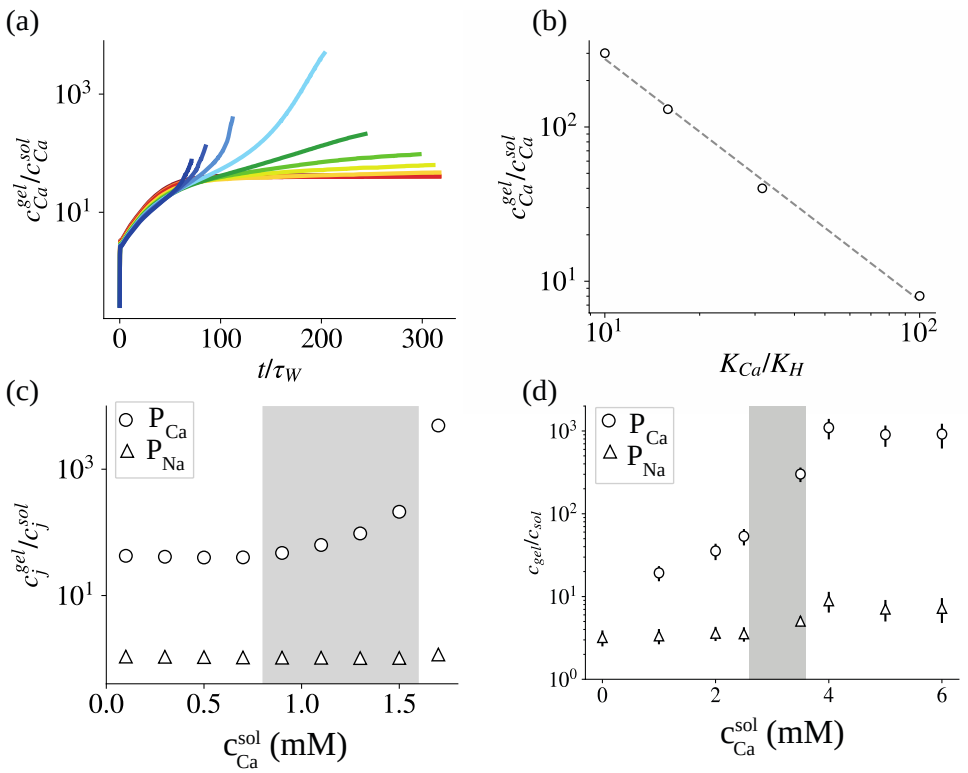

Figure 4: (a) Partition of calcium ions as a function of time for different values of initial concentration of calcium in the external bath solution (color code similar to figures 2a and 3a). (b) Calcium ion partition as a function of $K_{Ca}\left(=\frac{k_{Ca}^-}{k_{Ca}^+}\right)$ *upon starting with 0.5 mM* $CaCl_2$ *in the external bath solution (other parameters are similar to previous graphs). (c) Calcium (circles) and sodium (triangles) partition at last time-step of calculation (approximately "equilibrium"). (d) Ion partition coefficient measured for NaPA gels brought in equilibrium with an aqueous solution at pH = 5.5, containing 40 mM NaCl, and different concentrations of* $CaCl_2$ [5].

Movies S3 and S4 display the time evolution of free and adsorbed sodium and calcium ions in the system upon starting with initial conditions of 0.3 and 1.7 mM $CaCl_2$ in the external bath solution, respectively. To capture the weak attraction of monovalent cations to the polymer chains, we use relatively high desorption rate of the sodium ions and relatively low adsorption rate. Therefore, as solvent diffuses into the polymer network sodium ions are freed from the polymer attraction almost instantaneously (normalized time scale used in the simulation is $\frac{\tau_{Na}^-}{\tau_w} \sim 10^{-4}$). Subsequently only the calcium ions are adsorbed onto the polymer chains at a rate determined by the calcium adsorption coefficient. Electroneutrality is, of course, always satisfied.

The ion partition value is strongly influenced by the equilibrium adsorption coefficient $K_j = k_j^-/k_j^+$. Figure 4b demonstrates a linear dependence between K_{Ca} and $\frac{c_{Ca}^{gel}}{c_{Ca}^{sol}}$. Thus, we may be able to estimate the value of the equilibrium adsorption coefficient by measuring the partitioning response of the gel. Figure 4c compares the calcium (circles) and sodium (triangles) partition at the final time-step of calculation, which represents the equilibrium state for the swollen gels. Both cations partitioning coefficients increase monotonically upon increasing the concentration of calcium ions in the external bath solution. Sodium ion partitioning ranges between 1—10,

while calcium ion partitioning ranges between $10^1 - 10^3$. Figure 4d shows the ion partitioning measured for NaPA gels [5]. The trend of monotonic increase and order of magnitude are captured by the model calculation. For larger concentration of calcium ions (larger than c_1), the calcium partitioning seems to saturate or decrease slightly. Unfortunately, using the model we were unable to obtain equilibrium values for the collapsed phase in the regime of high calcium concentration. Thus, we can only conjecture that this behavior might be explained by competing trends between the capacity of the gel to adsorb calcium ions and increasing the calcium concentration in the external bath solution (the denominator of P_{Ca}).

As a final demonstration of the model capabilities, we study the effect of increasing the elastic modulus on the equilibrium degree of swelling. This is an example how the model may be used to predict effects of different internal and environmental parameters. Figure 5a indicates that increasing the elastic modulus causes a monotonic decrease in the degree of swelling of gels that are not completely collapsed ($c_{Ca} \leq c_1$), with no observable effect on the transition region, namely, the values of c_0 and c_1. Figure 5b shows measurements made on NaPA gels prepared with different crosslink densities [25]. According to the classical rubber elasticity theory the elastic constant, G_0, is linearly proportional to the crosslink density [44]. The effect of the elastic modifications on the equilibrium degree of swelling according to the model is qualitative comparable to the measurements.

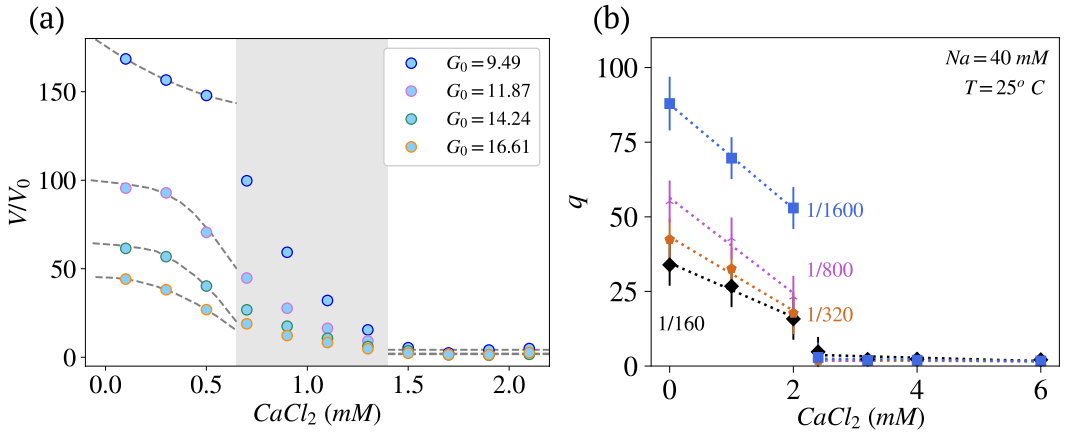

Figure 5: (a) Model calculation of the degree of swelling as a function of initial calcium ion concentration in the external bath solution for different values of the elastic modulus G_0. $k_{Ca}^- = 10^{-2}$ was used. Other parameters are the same as in figure 2. (b) Measurement of the degree of swelling as a function of calcium ion concentration in NaPA gels prepared with different crosslink densities. Average number of monomer units per crosslinker is 160, 320, 800, and 1600, respectively.

4 Conclusions

We have numerically investigated the predictions of a multicomponent fluid model describing the transient response of an anionic (i.e., negatively charged) polyelectrolyte hydrogel exposed to a new ionic environment consisting of monovalent and divalent cations. This model is based on principles that have a fundamental physical interpretation, including the conservation of mass and momentum, electroneutrality, Flory-Rehner theory of mixing crosslinked polymers and solvent molecules, Nernst–Planck model, and the law of mass action [36]. Our investigation sheds light on the coupled dynamics of the system components in a realistic non-equilibrium

scenario, which is closely connected and complements experimental work made on NaPA gels. For example, it is difficult to observe the dynamics of ion competition and adsorption onto the polymer chains with even the most sensitive detectors. However, the ionic behavior and its effect on the gel system – particularly on the Flory interaction parameter – can be described in unprecedented detail in computational simulation.

In turn, the experimental system provides crucial data (e.g., state diagrams), which are needed to keep the simulation as close as possible to reality. For example, in this work we used the simplest dependence of the interaction parameter χ on local concentration of adsorbed calcium ions. However, based on past experimental work the ionic dependence is believed to be more complex [24,34]. The modular nature of the model allows replacing a particular expression (e.g., equations S17-S18) with a more accurate one; e.g., as extracted from measurements. Thus, the model can become more precise by improving our understanding on certain constitutive relations. In particular, the Flory interaction parameter is modified by all types of ions (including monovalent cations) and not only by calcium ions [45]. Testing the constitutive model, namely, the linear dependence of the Flory parameter on the concentration of absorbed ions is crucial. Although it is difficult to directly probe this behavior, Molecular Dynamics simulations may be useful in predicting a more realistic relation between adsorbed ion concentration and the Flory interaction parameter [46].

While a continuum model of polymer-solvent-ion interactions does not provide the atomic or molecular specificity of an MD model, these are limited to describing processes occurring over nanometer length scales and at timescales ranging from picoseconds to nanoseconds. Their utility is limited when modeling processes like swelling and deswelling, which can occur over macroscopic length scales and over timescales ranging from milliseconds to hours to days. Using well-established polymer science concepts and explicitly imposing conservation laws leads to a satisfying compromise that is grounded in physics and polymer chemistry, but well suited to modeling water-ion-gel behavior at relevant scales. Of particular interest is the application of polymer science to biological polyelectrolytes at physiological ionic conditions, which is often not considered.

In the present work we focused on two important characteristic time scales: water diffusion and calcium adsorption onto the anionic polymer chains. While the former is well known, experimental data is scarce regarding the latter. Our estimation that at physiological conditions the adsorption rate of calcium ions acts at similar order of magnitude as the water diffusion leads to the prediction that partially dry gels swell significantly when exposed to solution containing a high concentration of divalent ions, and only subsequently collapse due to the divalent cation adsorption (figure 1a). This counterintuitive response is indeed validated experimentally (figure 2c).

Another important characteristic time – which was not the focus of this work – is the adsorption of hydrogen (or hydronium) ions onto the polymer chains. Hydrogen ions play an interesting role when competing with calcium ions – both are prone for adsorption and charge screening; e.g., in gastric mucus [37] – that would be worth studying in the future. Another

important time scale determines the re-organization of ions due to the electrical force and leads to electroneutrality. This characteristic time is determined from Ampere's and Gauss' laws and is ~10 ns; i.e., the ions are very quickly equilibrating in response to structural changes of the polymer chains, and as long as we are not modeling behaviors in the MHz regime, this approximation is expected to hold.

Despite the simplifying assumptions associated with the mean-field limit, the model requires the specification of four physical values (equation S24) and 23 dimensionless parameters (Table S1). While some of the model parameters are either known (ion diffusion coefficient) or can be reasonably estimated (average length of chains, fluid viscosity), the value of several parameters is generally not known *a priori* (e.g., solvent-network drag coefficient, ion adsorption and desorption coefficients). Thus, comparison of the model predictions to both kinetic and equilibrium swelling data can provide a good test to estimate the model parameters. For example, using a realistic value of the elastic modulus (≈10-100 kPa for NaPA gels) swollen gels fill the entire simulated space (L). Chain hydrophobicity, chain flexibility, chemical details (including specific interactions), etc., are critically important factors defining the interaction between polyelectrolyte chains, ions, and solvent molecules. These properties also affect the value of the elastic modulus [35]. Unfortunately, existing polyelectrolyte theories do not provide a reasonable estimate of the relative contributions of the above factors. It is likely that using more accurate values of other model parameters would resolve this apparent discrepancy.

Acknowledgements

We thank Alexandros Chremos, Nathan Hu Williamson, Velencia Witherspoon, and Rea Ravin for fruitful discussions. MM thanks Sinisa Pajevic for assistance with running the calculations at the NIH High Performing Computation (HPC) Biowulf cluster. MM, PJB, and FH acknowledge support by the Intramural Research Program of the *Eunice Kennedy Shriver* National Institute of Child Health and Human Development, NIH. OL acknowledges funding by NIH grant 5R01GM131408-04.

References

[1] M. Muthukumar, *50th Anniversary Perspective: A Perspective on Polyelectrolyte Solutions*, Macromolecules **50**, 9528 (2017).

[2] Y. Li and T. Tanaka, *Phase Transitions of Gels*, Annual Review of Materials Science **22**, 243 (1992).

[3] J. F. Joanny and J. Prost, *Active Gels as a Description of the Actin-Myosin Cytoskeleton*, HFSP Journal **3**, 94 (2009).

[4] P. Verdugo, *Supramolecular Dynamics of Mucus*, Cold Spring Harbor Perspectives in Medicine **2**, a009597 (2012).

[5] M. Mussel, P. J. Basser, and F. Horkay, *Ion-Induced Volume Transition in Gels and Its Role in Biology*, Gels **7**, 1 (2021).

[6] P. Calvert, *Hydrogels for Soft Machines*, Advanced Materials **21**, 743 (2009).
[7] H. Li, *Smart Hydrogel Modelling* (Springer, 2009).
[8] Y. I. Yang, Q. Shao, J. Zhang, L. Yang, and Y. Q. Gao, *Enhanced Sampling in Molecular Dynamics*, The Journal of Chemical Physics **151**, 70902 (2019).
[9] D. Hariharan and N. A. Peppas, *Modelling of Water Transport in Ionic Hydrophilic Polymers*, Journal of Polymer Science Part B: Polymer Physics **32**, 1093 (1994).
[10] D. J. Segalman and W. R. Witkowski, *Two-Dimensional Finite Element Analysis of a Polymer Gel Drug Delivery System*, Materials Science and Engineering: C **2**, 243 (1995).
[11] E. C. Achilleos, R. K. Prud'Homme, I. G. Kevrekidis, K. N. Christodoulou, and K. R. Gee, *Quantifying Deformation in Gel Swelling: Experiments and Simulations*, AIChE Journal **46**, 2128 (2000).
[12] E. C. Achilleos, K. N. Christodoulou, and I. G. Kevrekidis, *A Transport Model for Swelling of Polyelectrolyte Gels in Simple and Complex Geometries*, Computational and Theoretical Polymer Science **11**, 63 (2001).
[13] L. Feng, Y. Jia, X. Chen, X. Li, and L. An, *A Multiphasic Model for the Volume Change of Polyelectrolyte Hydrogels*, The Journal of Chemical Physics **133**, 114904 (2010).
[14] A. D. Drozdov and J. Declaville Christiansen, *Modeling the Effects of PH and Ionic Strength on Swelling of Polyelectrolyte Gels*, Journal of Chemical Physics **142**, 114904 (2015).
[15] Y. Mori, H. Chen, C. Micek, and M. C. Calderer, *A Dynamic Model of Polyelectrolyte Gels*, SIAM Journal on Applied Mathematics **73**, 104 (2013).
[16] V. V. Yashin and A. C. Balazs, *Theoretical and Computational Modeling of Self-Oscillating Polymer Gels*, Journal of Chemical Physics **126**, 124707 (2007).
[17] Y. Yu, C. M. Landis, and R. Huang, *Salt-Induced Swelling and Volume Phase Transition of Polyelectrolyte Gels*, Journal of Applied Mechanics, Transactions ASME **84**, (2017).
[18] G. L. Celora, M. G. Hennessy, A. Münch, B. Wagner, and S. L. Waters, *A Kinetic Model of a Polyelectrolyte Gel Undergoing Phase Separation*, Journal of the Mechanics and Physics of Solids **160**, 104771 (2022).
[19] F. Horkay, I. Tasaki, and P. J. Basser, *Osmotic Swelling of Polyacrylate Hydrogels in Physiological Salt Solutions*, Biomacromolecules **1**, 84 (2000).
[20] F. Horkay, P. J. Basser, A. M. Hecht, and E. Geissler, *Osmotic and SANS Observations on Sodium Polyacrylate Hydrogels in Physiological Salt Solutions*, Macromolecules **33**, 8329 (2000).
[21] F. Horkay, I. Tasaki, and P. J. Basser, *Effect of Monovalent-Divalent Cation Exchange on the Swelling of Polyacrylate Hydrogels in Physiological Salt Solutions*, Biomacromolecules **2**, 195 (2001).
[22] F. Horkay and P. J. Basser, *Ionic and PH Effects on the Osmotic Properties and Structure of Polyelectrolyte Gels*, Journal of Polymer Science Part B: Polymer Physics **46**, 2803 (2008).
[23] F. Horkay, A. M. Hecht, C. Rochas, P. J. Basser, and E. Geissler, *Anomalous Small Angle X-Ray Scattering Determination of Ion Distribution around a Polyelectrolyte Biopolymer in Salt Solution*, Journal of Chemical Physics **125**, 234904 (2006).
[24] M. Mussel, P. J. Basser, and F. Horkay, *Effects of Mono- and Divalent Cations on the Structure and Thermodynamic Properties of Polyelectrolyte Gels*, Soft Matter **15**, 4153 (2019).

[25] M. Mussel and F. Horkay, *Experimental Evidence for Universal Behavior of Ion-Induced Volume Phase Transition in Sodium Polyacrylate Gels*, Journal of Physical Chemistry Letters **10**, (2019).
[26] P. Verdugo, *Polymer Gel Phase Transition in Condensation-Decondensation of Secretory Products*, Advances in Polymer Science **110**, 145 (1993).
[27] I. Morfin, F. Horkay, P. J. Basser, F. Bley, A. M. Hecht, C. Rochas, and E. Geissler, *Adsorption of Divalent Cations on DNA.*, Biophysical Journal **87**, 2897 (2004).
[28] F. Horkay, P. J. Basser, A.-M. Hecht, and E. Geissler, *Effect of Calcium/Sodium Ion Exchange on the Osmotic Properties and Structure of Polyelectrolyte Gels*, Proceedings of the Institution of Mechanical Engineers, Part H: Journal of Engineering in Medicine **229**, 895 (2015).
[29] M. A. Zwieniecki, P. J. Melcher, and N. M. Holbrook, *Hydrogel Control of Xylem Hydraulic Resistance in Plants*, Science **291**, 1059 (2001).
[30] T. Wallmersperger, B. Kröplin, and R. W. Gülch, *Coupled Chemo-Electro-Mechanical Formulation for Ionic Polymer Gels----Numerical and Experimental Investigations*, Mechanics of Materials **36**, 411 (2004).
[31] H. Guo, T. Kurokawa, M. Takahata, W. Hong, Y. Katsuyama, F. Luo, J. Ahmed, T. Nakajima, T. Nonoyama, and J. P. Gong, *Quantitative Observation of Electric Potential Distribution of Brittle Polyelectrolyte Hydrogels Using Microelectrode Technique*, Macromolecules **49**, 3100 (2016).
[32] Y. D. Zaroslov, O. E. Philippova, and A. R. Khokhlov, *Change of Elastic Modulus of Strongly Charged Hydrogels at the Collapse Transition*, Macromolecules **32**, 1508 (1999).
[33] M. Mussel, E. Wilczynski, U. Eliav, J. Gottesman, M. Wilk, and U. Nevo, *Dynamics of Water and Sodium in Gels under Salt-Induced Phase Transition*, Journal of Polymer Science, Part B: Polymer Physics **53**, (2015).
[34] F. Horkay and P. J. Basser, *Osmotic Observations on Chemically Cross-Linked DNA Gels in Physiological Salt Solutions*, Biomacromolecules **5**, 232 (2004).
[35] J. Hua, M. K. Mitra, and M. Muthukumar, *Theory of Volume Transition in Polyelectrolyte Gels with Charge Regularization*, The Journal of Chemical Physics **136**, 134901 (2012).
[36] S. Sircar, J. P. Keener, and A. L. Fogelson, *The Effect of Divalent vs. Monovalent Ions on the Swelling of Mucin-like Polyelectrolyte Gels: Governing Equations and Equilibrium Analysis*, Journal of Chemical Physics **138**, 14901 (2013).
[37] O. L. Lewis, J. P. Keener, and A. L. Fogelson, *Electrodiffusion-Mediated Swelling of a Two-Phase Gel Model of Gastric Mucus*, Gels **4**, 76 (2018).
[38] *See Supplemental Material at [URL Will Be Inserted by Publisher].*, (n.d.).
[39] C. Alvarez-Lorenzo, O. Guney, T. Oya, Y. Sakai, M. Kobayashi, T. Enoki, Y. Takeoka, T. Ishibashi, K. Kuroda, K. Tanaka, G. Wang, A. Y. Grosberg, S. Masamune, and T. Tanaka, *Reversible Adsorption of Calcium Ions by Imprinted Temperature Sensitive Gels*, The Journal of Chemical Physics **114**, 2812 (2001).
[40] J. Du, O. L. Lewis, J. P. Keener, and A. L. Fogelson, *Modeling and Simulation of the Ion-Binding-Mediated Swelling Dynamics of Mucin-like Polyelectrolyte Gels*, (2021).
[41] P. J. Flory and J. Rehner, *Statistical Mechanics of Cross-Linked Polymer Networks II. Swelling*, The Journal of Chemical Physics **11**, 521 (1943).

[42] R. J. LeVeque, *Finite Volume Methods for Hyperbolic Problems*, Finite Volume Methods for Hyperbolic Problems (2002).
[43] V. Camacho, A. Fogelson, and J. Keener, *Eulerian--Lagrangian Treatment of Nondilute Two-Phase Gels*, Http://Dx.Doi.Org/10.1137/15M1023579 **76**, 341 (2016).
[44] P. J. Flory, *Principles of Polymer Chemistry* (Cornell University Press, 1953).
[45] D. W. Yin, F. Horkay, J. F. Douglas, and J. J. de Pablo, *Molecular Simulation of the Swelling of Polyelectrolyte Gels by Monovalent and Divalent Counterions*, Journal of Chemical Physics **129**, (2008).
[46] W. Zhang, E. D. Gomez, and S. T. Milner, *Predicting Flory-Huggins χ from Simulations*, Physical Review Letters **119**, 017801 (2017).
[47] K. Masatsuka, *I Do Like CFD, Vol. 1*, Vol. 1 (Lulu. com, 2013).
[48] J. Du, A. L. Fogelson, and G. B. Wright, *A Parallel Computational Method for Simulating Two-Phase Gel Dynamics on a Staggered Grid*, International Journal for Numerical Methods in Fluids **60**, 633 (2009).
[49] J. P. Keener, S. Sircar, and A. L. Fogelson, *Influence of the Standard Free Energy on Swelling Kinetics of Gels*, Physical Review E **83**, 41802 (2011).
[50] J. P. Celli, B. S. Turner, N. H. Afdhal, R. H. Ewoldt, G. H. McKinley, R. Bansil, and S. Erramilli, *Rheology of Gastric Mucin Exhibits a PH-Dependent Sol-Gel Transition*, Biomacromolecules **8**, 1580 (2007).
[51] L. Alves, B. Lindman, B. Klotz, A. Böttcher, H.-M. Haake, and F. E. Antunes, *Rheology of Polyacrylate Systems Depends Strongly on Architecture*, (n.d.).
[52] S. Schreiber and P. Scheid, *Gastric Mucus of the Guinea Pig: Proton Carrier and Diffusion Barrier*, Https://Doi.Org/10.1152/Ajpgi.1997.272.1.G63 **272**, (1997).
[53] B. D. E. Raynal, T. E. Hardingham, J. K. Sheehan, and D. J. Thornton, *Calcium-Dependent Protein Interactions in MUC5B Provide Reversible Cross-Links in Salivary Mucus **, Journal of Biological Chemistry **278**, 28703 (2003).